Soft Matter

PAPER

Switching periodic membranes *via* pattern transformation and shape memory effect†

Jie Li,[a] Jongmin Shim,[b] Justin Deng,[c] Johannes T. B. Overvelde,[b] Xuelian Zhu,[a] Katia Bertoldi[b] and Shu Yang*[a]

We exploited mechanical instability in shape memory polymer (SMP) membranes consisting of a hexagonal array of micron-sized circular holes and demonstrated dramatic color switching as a result of pattern transformation. When hot-pressed, the circular holes were deformed to an array of elliptical slits (with width of tens of nanometers), and further to a featureless surface with increasing applied strain, therefore, switching the membrane with diffraction color to a transparent film. The deformed pattern and the resulting color change can be fixed at room temperature, both of which could be recovered upon reheating. Using continuum mechanical analyses, we modeled the pattern transformation and recovery processes, including the deformation, the cooling step, and the complete recovery of the microstructure, which corroborated well with experimental observations. We find that the elastic energy is roughly two-orders of magnitude larger than the surface energy in our system, leading to autonomous recovery of the structural color upon reheating. Furthermore, we demonstrated two potential applications of the color switching in the SMP periodic membranes by (1) temporarily erasing a pre-fabricated "Penn" logo in the film *via* hot-pressing and (2) temporarily displaying a "Penn" logo by hot-pressing the film against a stamp. In both scenarios, the original color displays can be recovered.

Introduction

Shape memory polymers (SMPs) are polymeric smart materials of interest for a variety of applications, including deployable space structures, artificial muscles, biomedical devices, sensors, smart dry adhesives, and fasteners.[1,2] They form a "permanent" shape by chemical or physical crosslinking (*e.g.* crystallization or chain entanglement). Above a thermal phase transition temperature, either a glass transition temperature (T_g) or a melting temperature (T_m), SMPs can be deformed to different temporary shapes, which can be fixed by cooling the sample. Upon exposure to an external stimulus, such as heat, light, and solvent, the temporary shapes can return to their original (or the permanent) shape. There has been much effort to develop new chemistry for improved shape fixity and shape recovery efficiency, responsiveness to new environmental triggers, achieving a multi-shape memory effect, and applications to biomedical devices.[1,3–9] Nevertheless, most of the studies focus on the shape memory effect in bulk SMPs. A few groups have created micropatterns in SMPs, such as microprotrusions[10] and microwrinkles[8,11] by taking advantage of the large modulus change near the phase transition temperature. None of them, however, have reported the recovery to the original shape from the micropatterns. During the shape recovery process, the entropic energy stored in the deformed state is released. It remains to be seen whether the deformed shape can be completely recovered as the surface energy becomes increasingly dominant when the size shrinks to micro- and nanoscale.

Recently, we and several other groups have demonstrated pattern transformation in elastic membranes of periodic hole arrays by mechanical compression,[12,13] solvent swelling,[14,15] polymerization,[16] and capillary force.[17] For example, when swollen by an organic solvent, a poly(dimethylsiloxane) (PDMS) membrane consisting of micron-sized circular holes in a square array buckles to a diamond plate pattern of elliptic slits with the neighboring units perpendicular to each other.[14] As a result, the physical properties (*e.g.* photonic[18,19] and phononic[15] band gaps[18,19] and mechanical behaviors[20,21]) could be significantly altered due to the change of lattice symmetry, pore size, shape and volume filling fraction. One question rises whether it is

[a]Department of Materials Science and Engineering, University of Pennsylvania, 3231 Walnut Street, Philadelphia, PA 19104, USA. E-mail: shuyang@seas.upenn.edu; Fax: +1-215-573-2128; Tel: +1-215-898-9645

[b]School of Engineering and Applied Science, Harvard University, Cambridge, MA 02138, USA. E-mail: bertoldi@seas.harvard.edu

[c]Department of Materials Science and Engineering, Cornell University, Bard Hall, Ithaca, NY 14853, USA

possible to switch a colorful film to a transparent one *via* pattern transformation. The latter state will allow for seeing through or mingling with the surroundings. Therefore, the dramatic visual contrast between colored and transparent states is of interest for applications such as displays, privacy windows, and camouflages. In nature, invisibility is an important strategy for many sea creatures to hide from predators in water. For example, bobtail squids are invisible in sand during the day with chromatophores in the skin concentrated into small, barely visible dots; when the muscle fibers stretch out the skin, thereby enlarging the chromatophores, the color becomes visible for signaling or escape from predators.[22]

Here we report on switching of a SMP membrane with diffraction color to a transparent film *via* harnessing the mechanical instability and the shape memory effect. When hot-pressed, the SMP membrane consisting of a hexagonal array of circular holes (1.2 μm diameter, 2.5 μm pitch, and 5.0 μm depth) underwent pattern transformation from an array of elliptical slits to a featureless surface with increasing applied strain, leading to a dramatic change of the hole size and shape, and diffraction color, which could be fixed at room temperature, and later recovered to the original pattern (and color) upon reheating. Using continuum mechanical analyses, we modeled, for the first time, an out-of-plane compression of the SMP membrane. We observed the hot-press induced deformation and pattern transformation of the membrane at different strains, the structure fixation at the cooling step, and the complete recovery of the microstructure, in agreement with experiments. We also find that the elastic energy stored in the membrane is roughly 2-orders of magnitude larger than the surface energy, leading to autonomous recovery of the structural color upon reheating. Further, we demonstrated two possible applications of color and transparency change in our SMP periodic membranes, including (1) temporary erasing of the pre-fabricated "Penn" logo in the film and (2) a temporary display of the "Penn" logo by hot-pressing the film against a stamp.

Results and discussion

The ability to simultaneously change the lattice symmetry, pore size and shape, and volume filling fraction through pattern transformation offers an attractive approach to drastically alter the materials properties. Most deformation methods reported so far involve the use of solvent, either through swelling or drying processes. In comparison, application of a mechanical force will allow us to independently control the amount, direction (uniaxial or biaxial both in-plane and out-of-plane), and timing of strain applied to the periodic structures. In the case of in-plane compression, however, additional care has to be taken to eliminate the out-of-plane buckling, *e.g.* by sandwiching the film between two rigid sheets.[12] In most applications, a direct out-of-plane compression is easy to implement and desirable, and was thus performed in our experiments.

Color/transparency switching in SMP periodic membranes

The SMP periodic membrane (1.2 μm diameter, 2.5 μm pitch, and 5 μm depth) was prepared by replica-molding from a 2D hexagonal pillar array, which was fabricated by 3-beam

holographic lithography[23,24] (see Fig. 1a and b and details in the Experimental section). The negative-tone photoresist, epoxy-cyclohexyl POSS® cage mixture (epoxy POSS), was chosen here to fabricate the pillar array since it could be readily removed by hydrofluoric acid (HF) solution at room temperature[23] after templating the SMP membrane. When the latter was heated to 10–30 °C above its T_g (70 °C), it became softened and was compressed vertically by a hot-press to a temporary shape (Fig. 1c). The load was carefully controlled to deform the membrane at different strain levels, here referring to engineering strain, ε = change of film thickness/original thickness. The temporary shape was fixed when cooled down to room temperature while keeping the loading force constant. Upon reheating to 90 °C, the hexagonal shape was recovered. During the pattern deformation and recovery, we observed reversible switching of color and transparency.

Although the bulk SMP film is transparent, the SMP membrane is colorful due to the diffraction grating effect (Fig. 2a, f and k). Because of the Gaussian distribution of the laser beam in holographic lithography and possible small misalignment of optics, there was a gradient laser intensity from center to the edge, resulting in pore size distribution and color variation across the sample size. This can be improved using a beam shaper or patterning the film by conventional photolithography through a photomask. When the applied strain, ε, was ~13 ± 2%, the circular holes of *p6mm* symmetry were deformed to elliptical slits (width of major axis 1.25 μm and minor axis 500 nm) with *p2gg* symmetry (Fig. 2g and l), in agreement with the observation from the swelling-induced instability in SU-8 membranes with a hexagonal array of pores.[15] When the SMP membrane was compressed in the vertical direction, it expanded in-plane due to positive Poisson's ratio, hence generating an equivalent in-plane compressive stress to the circular holes. The initial diffraction color
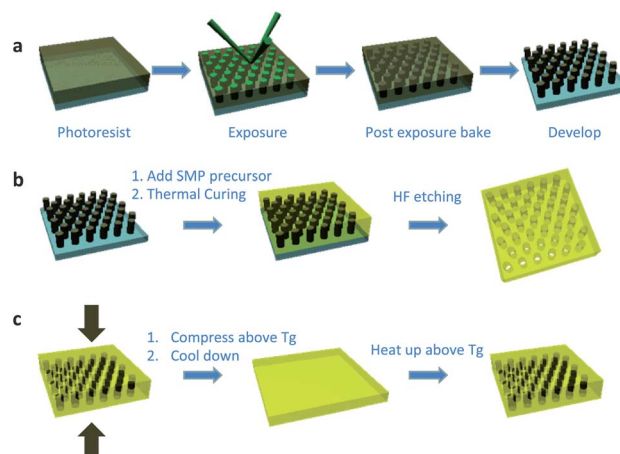

Fig. 1 Schematic illustration of fabrication and deformation/recovery of a 2D SMP membrane. (a) Fabrication of a 2D pillar array by holographic lithography. (b) Fabrication of the SMP membrane with periodic holes by replica molding, followed by etching in HF aqueous solution. (c) Hot-pressing of the SMP membrane in the vertical direction above T_g. The temporary shape could be fixed by cooling down to room temperature under the load. The original shape could be recovered upon reheating above T_g.
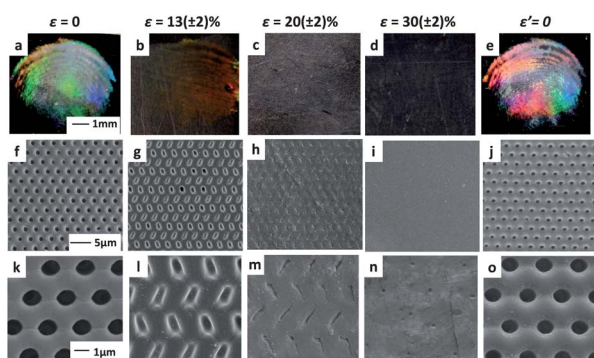
Fig. 2 Pattern transformation and recovery in a 2D SMP membrane. Optical images of the: original (a); partially deformed, $\varepsilon \sim 13 \pm 2\%$ (b) and $\varepsilon \sim 20 \pm 2\%$ (c); completely deformed, $\varepsilon \sim 30 \pm 2\%$ (d); and recovered SMP membranes (e). (f–j) Corresponding SEM images of the SMP membranes shown in (a–e). (k–o) Higher magnification SEM images of (f–j).

diminished significantly after compression although it was not completely lost at this strain level (Fig. 2b). This could be attributed to the smaller pore size and porosity. The width of the minor axes of the ellipse further decreased, from hundreds of nanometers to a few nanometers, as the strain was increased. When ε was increased to $\sim 20 \pm 2\%$, the holes were almost closed into lines (see Fig. 2c, h and m) and the SMP membrane became quite transparent, much like the bulk film. At $\varepsilon \sim 30 \pm 2\%$, the holes were closed-up and the surface became nearly featureless (Fig. 2d, i and n). No further change of transparency was observed. When any of the above deformed SMP membranes were reheated to 90 °C, the original periodic structure was restored nearly to completion (97.6% of the original hole size and 100% of the original pitch), as evident by the SEM images and the regeneration of strong diffraction color (Fig. 2e, j and o and Movie S1†). Surprisingly, even the one with completely closed pores was restored, suggesting that the adhesive energy between the pore surfaces was much smaller than the elastic recovery energy. The different colors displayed in Fig. 2a (the original film) and Fig. 2e (the recovered one) could be caused by a small misalignment of incident light during photo shooting which could lead to appearance of a different color. When ε was greater than 50%, the 2D grating with air holes and its color could no longer be completely recovered due to the permanent deformation of the polymer network.

The reversible switching between the colorful displays to transparency was repeated successfully for more than 10 cycles with $\varepsilon < 50\%$, and the recovery of diffraction color occurred within a few seconds (see Movie S1†). According to SEM images, the hole diameter and pitch of the recovered film decreased slightly to 94.4% and 98.4% of the original one, respectively, after three cycles and to 89.7% and 98.0% of the original one, respectively, after ten cycles. The diffraction color displayed at any of the temporary states could be reprogrammed *on demand* by precise control of the applied strain level and temperature/ load of deformation. Hence, it is possible to build a color spectrum by carefully tuning the mechanical deformation. Further, we may achieve a full-color display by combining the instability and design of the original microstructures with variable structural parameters.

During the pattern transformation and recovery processes, the air holes were squeezed out and restored, respectively, which would result in a dramatic transparency change. As a proof-of-concept, we placed two SMP membranes on a paper printed with "Penn" logos: one was hot-pressed at $\varepsilon \sim 30 \pm 2\%$ (the left one), and the other was the original, non-deformed one (the right one, see illustration in Fig. 3a). Due to diffraction from the surface of the original membrane with pores in a hexagonal array, the "Penn" letters beneath it could not be clearly viewed, in sharp contrast to that beneath the deformed membrane (see Fig. 3b). The transparency change was further investigated by UV-Vis spectroscopy at different thermal and mechanical treatments (Fig. 3c) using the bulk SMP film as a reference. As expected, the original sample (A) has the lowest transmittance (*e.g.* 28.1% at λ = 600 nm). For the hot-pressed samples, sample (B) that was deformed at $\varepsilon \sim 13 \pm 2\%$ shows improved transmittance, 46.9% at 600 nm, and the sample (C), which was deformed at $\varepsilon \sim 30 \pm 2\%$ with closed voids, has the highest transmittance, 88.8% at 600 nm, in comparison with the bulk SMP film. The slightly lowered transparency may be attributed to the surface roughness of the SMP membrane introduced by the Teflon sheets and dust particles trapped on the sample surface during hot-pressing and press release. Finally, the recovered sample (D) shows low transmittance (32.5% at 600 nm), close to that of the original membrane in the UV-visible region.
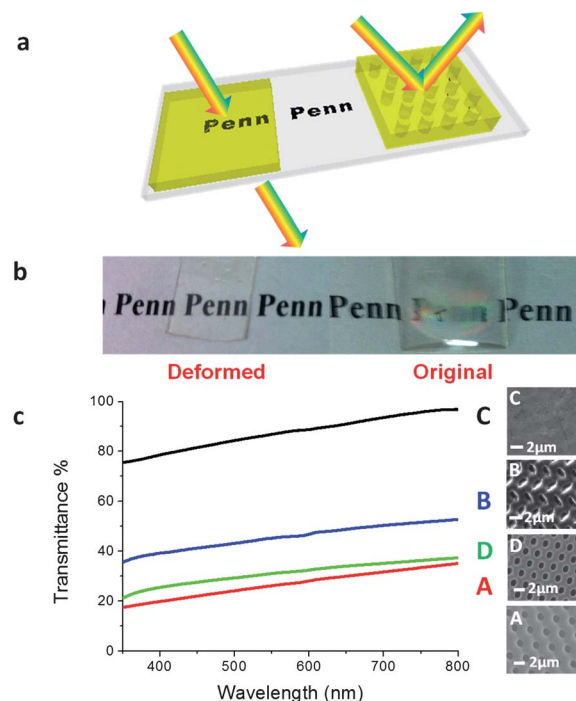

Fig. 3 Display of "Penn" logos underneath 2D SMP membranes. (a) Schematic illustration of transparency comparison between the deformed and the original SMP membranes. (b) Optical images of the deformed and original SMP membranes on top of the "Penn" logo. The "Penn" underneath the original membrane is hardly legible but clearly visible under the deformed sample. (c) UV-Vis spectra of different 2D SMP membranes (A–D) using the bulk SMP film as a reference. A. Original. B. Deformed at $\varepsilon \sim 13 \pm 2\%$. C. Deformed at $\varepsilon \sim 30 \pm 2\%$. D. Recovered one.

Finite element analysis

Since the deformation results presented here are the first demonstration of instabilities induced by loading in the direction perpendicular to the voids, we built a 3D mechanical model to quantitatively investigate the buckling and post-buckling behaviors. The structure is modeled as an infinite array of infinitely long voids in the x_1–x_2 plane. 3D analyses are conducted and the constraining effect given by the substrate is accounted for by setting the lateral expansion equal to zero. A periodic representative volume element (RVE), as shown in Fig. 4a, is considered and a series of constraint equations are applied to the boundaries of the model providing general periodic boundary conditions.

The stress–strain behavior of the SMP is captured using a two-mechanism constitutive model.[15] The stress response is decomposed into two contributions: the resistance due to stretching and orientation of the molecular network (σ_N), mechanism N, and the resistance due to intermolecular interactions (σ_v), mechanism V. At the applied temperature T, the total stress acting on the material is given by

$$\sigma = \sigma_N + V_v \sigma_v \qquad (1)$$

where $V_v = 1 - \dfrac{1}{1 + \exp\left[-\dfrac{T - T_g + A_1}{A_2}\right]}$ with A_1 and A_2 as

material parameters defining the position and width of the zone where mechanism V becomes significant.

The shape memory behavior is taken into account by having σ_v depend on $(T - T_g)$. When $T > T_g$ the material is characterized by a rubbery behavior; as T decreases toward T_g, the material becomes increasingly glassy and locked into the deformation. The constitutive model is implemented into a user-defined subroutine (VUMAT) of the commercial finite element code ABAQUS, and numerical simulations of the whole thermo-mechanical loading history of the structures are performed in four steps (see Fig. 4 and Movie S2†) using the model parameters summarized in Table 1.
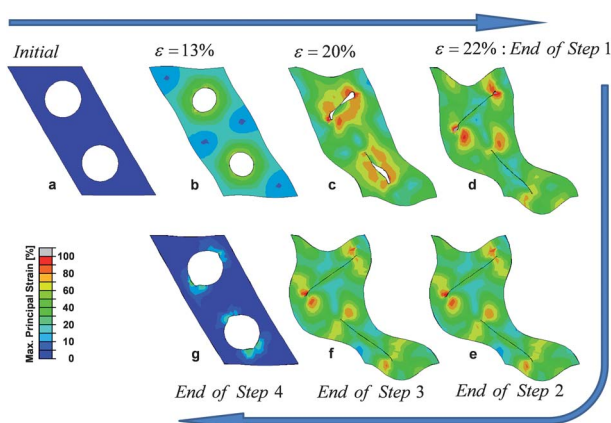
Step (1) *Hot-pressing*. T increases above T_g, so that σ_v vanishes and the material exhibits rubber-like behavior. The stability of the structure is investigated by conducting a Bloch wave analysis.[25] At an applied strain, $\varepsilon = 11\%$, a critical instability is detected, leading to the same pattern previously observed under constrained swelling,[15] which is characterized by sheared voids where the shear direction alternates back and forth from row to row (see Fig. 4a–c). Further compression leads to complete closure of the voids at $\varepsilon = 22\%$ (Fig. 4d), in agreement with experimental observation (Fig. 2h). In the simulations, further compression was avoided to prevent too much mesh distortion.

Step (2) *Cooling down*. T decreases to 20 °C, and σ_v increases, making the material much stiffer and preserving the pattern (Fig. 4e).

Step (3) *Unloading*. The press is removed, but the holes remain completely closed (Fig. 4f), and the elastic energy is stored in the material.

Step (4) *Reheating up*. T increases above T_g so that the structure again exhibits a rubbery behavior (σ_v vanishes again) and the initial shape and pattern are elastically recovered (see Fig. 4g).

As seen in Fig. 4, the numerical analysis nicely captured the deformation, pattern transformation and recovery of the SMP structures. Moreover, the analysis revealed a strong dependency of the onset of instability on the porosity of the structure. Thus the discrepancy between experiments and simulations observed close to the onset of instability at $\varepsilon = 13\%$ (Fig. 2g and 4b) may be attributed to a small difference in porosity between the model and the tested sample. Additionally, we find that for the considered structures with voids of 1 μm diameter the surface energy (22.8 mJ m^{-2} measured by a goniometer) is roughly two orders of magnitude smaller than the elastic recovery energy, making the recovery autonomous upon reheating. Since the strain energy is proportional to L^3 (with L denoting the characteristic material dimension), while the surface energy is proportional to L^2, a decrease of the voids diameter will increase the contribution of the surface energy. An approximate analysis suggests that the surface energy will play an important role for voids 10 times smaller than those considered in this study.

Color displays with SMP periodic membranes

To demonstrate the flexibility of color and transparency change in our SMP periodic membranes and their potential applications,

Fig. 4 Numerical results for the SMP thermo-mechanical cycle. Snapshots of the hexagonal lattice during Step 1, hot-pressing at different strain levels (a–d), and at the end of Steps 2, cooling down (e), 3, unloading (f) and 4, reheating (g). The color gives an indication of the maximum principal strain distribution.

Table 1 Material constants for SMP used in the mechanical models[a]

Rubbery phase (mechanism N)	Glassy phase (mechanism V)	Temperature related constants
$\mu = 1.72$ MPa	$E = 1500$ MPa	$T_g = 343$ K
$N = 4.33$	$\nu = 0.45$	$A_1 = 20$ K
$K = 16.7$ MPa	$\dot{\gamma}_0 = 52 \times 10^6$ s^{-1}	$A_2 = 5$ K
	$\Delta G = 92 \times 10^{-21}$ J	
	$S_0 = 56$ MPa	
	$S_{ss} = 28$ MPa	
	$h = 400$ MPa	

[a] μ is the elastic shear modulus, N is the parameter related to the limiting chain extensibility, K is the bulk modulus, E is the Young's modulus, ν is Poisson's ratio, $\dot{\gamma}_0$ is the pre-exponential shear strain rate factor, ΔG is the activation energy, S_0 is the initial athermal deformation resistance, S_{ss} is the athermal deformation resistance value at the steady state, and h is the softening slope (the slope of the yield drop with respect to plastic strain).

we exploited two possible renderings of the SMP membranes. First, a "Penn" logo was pre-fabricated within the 2D membrane (Fig. 5a and b). The template for replica molding was fabricated by exposing the negative-tone photoresist, epoxy POSS, to UV light through a photomask with the "Penn" logo, followed by 3-beam holographic lithography to create a hexagonal array of pillars in the surrounding area (Fig. 5c). Since the region with "Penn" was mostly crosslinked in the first step, the second exposure did not produce any pillar in this region but shallow voids (Fig. 5d). After replica-molding the template to the SMP membrane, there was no or little color diffracted from this region in sharp contrast to the bright color from the surrounding area (Fig. 5e and g). When the SMP membrane was hot-pressed above T_g, the "Penn" logo disappeared as the film became transparent (Fig. 5f). When reheated, the "Penn" logo reappeared together with its colorful background, confirming the success of shape recovery. Here, the logo was pre-fabricated in the permanent shape, which could be temporarily erased upon deformation.

In a second approach, the "Penn" logo was introduced as a temporary shape by a rubber stamp indented into the SMP membrane during heating (Fig. 6a) at 90 °C. The stamp was released after the film was cooled down to room temperature. As seen in Fig. 6b and d, the indented region was transparent, especially at the sharp corners of the letters, presumably receiving higher stress, while the background remained colorful. When reheated, the "Penn" logo was erased (Fig. 6c and e). In this way, different letters or patterns could be "finger-printed" and reprogrammed into the same SMP membrane repeatedly, which could be extremely useful as a user-friendly touch screen display or fingerprinting by tailoring the SMP T_g near the body temperature. It should be noted that all the displays presented here require no extra energy to maintain the displayed state.
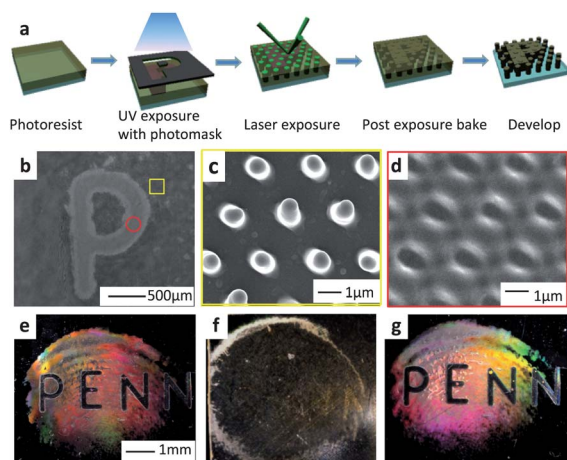

Fig. 5 Display of "PENN" embedded in a 2D SMP membrane. (a) Schematic illustration of the fabrication of the template. (b–d) SEM images of the photoresist template before replication to the SMP membrane. (b) A low magnification SEM image of the "P" character in the template. (c) SEM image of the structure outside "P" character, yellow square, showing tall pillars. (d) SEM image of the structure inside the "P" character, red circle, showing a nearly flat film with shallow voids. (e–g) Optical images of the original (e), deformed (f) and recovered (g) SMP films.
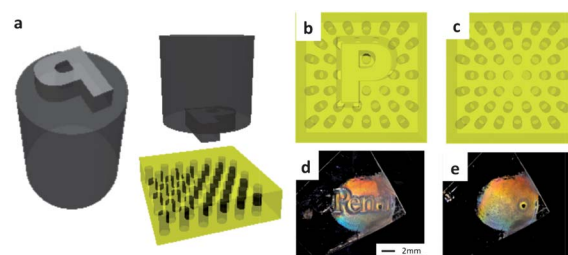

Fig. 6 Indentation display on the SMP membrane. Schematic illustrations of (a) indentation of a stamp with a letter "P" into a heated SMP membrane, (b) the display of the letter "P" in the SMP membrane in the deformed region and (c) structural recovery upon reheating. Corresponding optical images of the indented "Penn" in the colored SMP membrane (d) and its erase after reheating the SMP membrane to 90 °C (e).

Conclusions

We prepared a 2D periodic membrane in SMPs, and studied the mechanical instability and shape memory effect. When hot-pressed, the membrane underwent pattern transformation from a *p6mm* hexagonal lattice of circular holes (1 μm diameter) to a *p2gg* pattern of elliptical slits (widths varied from a few hundreds of nm to a few nm), and eventually the holes were completely closed. The original film is colorful because of the diffraction from the periodic micropattern and can be reversibly switched to a transparent state by mechanical deformation above the material's T_g. Upon reheating, the deformed patterns were able to recover, hence restoring the diffraction color. The combination of pattern transformation and shape memory effect in a 2D periodic membrane offers several distinctive characteristics. (1) It is the first demonstration of instabilities induced by loading in the direction perpendicular to the voids in microstructured SMPs, which is more desirable in practical applications than approaches such as solvent swelling and in-plane compression. (2) The temporarily deformed structure and the resulting color can be fixed without the need for continuous input of external trigger; they can also be programmed continuously by varying the mechanical strain level. (3) The continuum mechanical analyses have realistically captured the buckling and post-buckling behaviors of the SMP membrane observed experimentally. Importantly, the model suggests that the surface energy plays a negligible role compared with elastic energy when the void dimension is comparable to the wavelength of light, leading to autonomous and fast shape recovery of the microstructure.

We emphasize that while the diffraction color change is demonstrated in temperature responsive SMPs here, there are a broad range of stimuli responsive material systems in the literature, allowing for fine-tuning the transition temperature, switching speed, degree of responsiveness, number of temporary states, and the type of stimulus. For example, the T_g of the epoxy SMP used in our system could be lowered (*e.g.* to 30 °C) by increasing the concentration of a more flexible crosslinker, decylamine.[26] SMPs that can store up to three different shapes in temporary states have been reported.[7,27] We expect that the study of tuning periodic structures *via* combined pattern transformation and shape memory effect will shed new light into harnessing the mechanical response of soft materials and advancing a wide range of technologies, including color displays,

sensors, camouflage, and energy efficient building components (*e.g.* smart windows and responsive facades).

Experimental section

Unless specifically noted, all chemicals were obtained from Sigma-Aldrich (St Louis, MO, USA) and used as received.

Fabrication of the hexagonal pillar array (Fig. 1a)

The SMP periodic membrane was replica molded from a 2D hexagonal pillar array (1.2 μm diameter, 2.5 μm pitch, and 5 μm height), which was fabricated by 3-beam holographic lithography (HL)[23,24] from epoxycyclohexyl POSS® cage mixture (EP0408, Hybrid Plastics®) (epoxy POSS) mixed with a 0.9 wt% photoinitiator, Irgacure 261 (Ciba Specialty Chemicals). In a typical HL experiment, the epoxy POSS photoresist was spin-coated on a glass substrate, pre-baked at 50 °C for 40 min, followed by 95 °C for 2 min. The film was then exposed to three interfering laser beams ($\lambda = 532$ nm, power of beam source $\sim$1.0 W), followed by post-exposure bake (PEB) at 50 °C for 30 s (Fig. 1a). The pillar structures were obtained after development in propylene glycol methyl ether acetate (PGMEA), rinsing in isopropanol (IPA), followed by drying in a critical point dryer (SAMDRI®-PVT-3D, tousimis) from ethanol to prevent pillar collapse. The sample area was defined by the laser beam size, typically $\sim$1 cm diameter. By varying the dosage of laser exposure and the PEB time and temperature, we obtained hole sizes ranging from hundreds of nanometers to a few microns.

Replica molding SMP periodic membrane (Fig. 1b)

The SMP precursor, a mixture with molar ratio 5 : 1 : 3 of melted diglycidyl ether of bisphenol A epoxy (EPON 826), poly-(propylene glycol)bis(2-aminopropyl)ether (Jeffamine D-230) and decylamine (DA), was infiltrated into the template *via* capillarity at 50 °C followed by thermal curing at 100 °C for 1.5 h and 150 °C for 1 h, respectively. The T_g can be tuned from 40 °C to 90 °C by varying the ratio of difunctional D230 and mono-functional DA.[26] Here, the SMP was formulated to have a T_g of 70 °C. After crosslinking EPON 826, the epoxy POSS template and the glass substrate were etched away by aqueous HF solution (48 wt%), resulting in a free-standing SMP membrane of a hexagonal array of holes on a $\sim$500 μm thick bulk film.

Hot pressing of SMP membranes

The SMP membrane was compressed in the vertical direction using a manual bench top heated hydraulic press (CARVER 4122, Carver, Inc). The sample (>0.4 mm thick) was placed inside a Teflon sample holder (0.4 mm thick), which was then pressed between two Teflon sheets with heated platens. The platens were pre-heated to 100 °C for 10 min to reach equilibrium. Then a pressure of 1000 psi was applied to the sample and kept for 15 min before cooling down to room temperature, followed by release of the pressure to lock the temporary shape. The strain was calculated by comparing the final film thickness with the original one.

Fabrication of the SMP membrane with embedded "Penn" letter

The membrane was fabricated by replica molding in a way similar to that from the hexagonal POSS pillar array. One added step was UV exposure ($\lambda = 365$ nm, 400 mJ cm^{-2}, 97435 Oriel Flood Exposure Source, Newport) through a "Penn" logo photomask conducted after pre-baking and before the three-beam laser exposure. After PEB, the "Penn" region was highly crosslinked and appeared nearly flat or with shallow features depending on the dosage, while the surrounding areas formed pillar structures.

Calculation/modelling

Numerical simulations of stability of the structure were conducted using the nonlinear finite element code ABAQUS/Standard (version 6.8-2) while the thermo-mechanical loading history of the structures was investigated utilizing the nonlinear finite element code ABAQUS/Explicit (version 6.8-2). Each mesh was constructed of 8-node, linear, 3D elements (ABAQUS element type C3D8R). In the hexagonal array the voids have a radius $R = 1$ μm and a unit cell spanned by the lattice vectors $A_1 = $ [2 0 0] μm and $A_2 = $ [1 1.732 0] μm and $A_3 = $ [0 0 0.1] μm is used. An RVE consisting of $1 \times 2 \times 1$ unit cells is considered in the simulations of the thermo-mechanical loading cycle and an imperfection in the form of the most critical eigenmode is introduced into the mesh to capture the instability upon hot-pressing, the subsequent freezing-in of the transformed pattern and then the shape recovery behavior. The stress–strain behavior of the SMP is captured using the material parameters reported in Table 1.

Acknowledgements

Notes and references

1 A. Lendlein and R. Langer, *Science*, 2002, **296**, 1673.
2 C. Liu, H. Qin and P. T. Mather, *J. Mater. Chem.*, 2007, **17**, 1543.
3 A. Lendlein, H. Y. Jiang, O. Junger and R. Langer, *Nature*, 2005, **434**, 879.
4 J. M. Ortega, W. Small, T. S. Wilson, W. J. Benett, J. M. Loge and D. J. Maitland, *IEEE Trans. Biomed. Eng.*, 2007, **54**, 1722.
5 C. M. Yakacki, R. Shandas, D. Safranski, A. M. Ortega, K. Sassaman and K. Gall, *Adv. Funct. Mater.*, 2008, **18**, 2428.
6 T. Chung, A. Rorno-Uribe and P. T. Mather, *Macromolecules*, 2008, **41**, 184.

7 T. Xie, *Nature*, 2010, **464**, 267.
8 T. Xie, X. C. Xiao, J. J. Li and R. M. Wang, *Adv. Mater.*, 2010, **22**, 4390.
9 L. Sun and W. M. Huang, *Soft Matter*, 2010, **6**, 4403.
10 N. Liu, Q. Xie, W. M. Huang, S. J. Phee and N. Q. Guo, *J. Micromech. Microeng.*, 2008, **18**, 027001.
11 Y. Zhao, W. M. Huang and Y. Q. Fu, *J. Micromech. Microeng.*, 2011, **21**, 067007.
12 T. Mullin, S. Deschanel, K. Bertoldi and M. C. Boyce, *Phys. Rev. Lett.*, 2007, **99**, 084301.
13 S. Willshaw and T. Mullin, *Soft Matter*, 2012, **8**, 1747.
14 Y. Zhang, E. A. Matsumoto, A. Peter, P. C. Lin, R. D. Kamien and S. Yang, *Nano Lett.*, 2008, **8**, 1192.
15 J. H. Jang, C. Y. Koh, K. Bertoldi, M. C. Boyce and E. L. Thomas, *Nano Lett.*, 2009, **9**, 2113.
16 S. Singamaneni, K. Bertoldi, S. Chang, J. H. Jang, E. L. Thomas, M. C. Boyce and V. V. Tsukruk, *ACS Appl. Mater. Interfaces*, 2009, **1**, 42.
17 X. Zhu, G. Wu, R. Dong, C.-M. Chen and S. Yang, *Soft Matter*, 2012, **8**, 8088.
18 X. L. Zhu, Y. Zhang, D. Chandra, S. C. Cheng, J. M. Kikkawa and S. Yang, *Appl. Phys. Lett.*, 2008, **93**, 161911.
19 D. Krishnan and H. T. Johnson, *J. Mech. Phys. Solids*, 2009, **57**, 1500.
20 S. Singamaneni, K. Bertoldi, S. Chang, J. H. Jang, S. L. Young, E. L. Thomas, M. C. Boyce and V. V. Tsukruk, *Adv. Funct. Mater.*, 2009, **19**, 1426.
21 K. Bertoldi, P. M. Reis, S. Willshaw and T. Mullin, *Adv. Mater.*, 2010, **22**, 361.
22 M. Izumi, A. M. Sweeney, D. DeMartini, J. C. Weaver, M. L. Powers, A. Tao, T. V. Silvas, R. M. Kramer, W. J. Crookes-Goodson, L. M. Mathger, R. R. Naik, R. T. Hanlon and D. E. Morse, *J. R. Soc. Interface*, 2010, **7**, 549.
23 Y. Xu, X. Zhu and S. Yang, *ACS Nano*, 2009, **3**, 3251.
24 J. H. Moon, A. J. Kim, J. C. Crocker and S. Yang, *Adv. Mater.*, 2007, **19**, 2508.
25 K. Bertoldi, M. C. Boyce, S. Deschanel, S. M. Prange and T. Mullin, *J. Mech. Phys. Solids*, 2008, **56**, 2642.
26 T. Xie and I. A. Rousseau, *Polymer*, 2009, **50**, 1852.
27 I. Bellin, S. Kelch, R. Langer and A. Lendlein, *Proc. Natl. Acad. Sci. U. S. A.*, 2006, **103**, 18043.